

Supplementary Information

Towards covalent organic frameworks with predesignable and aligned open docking sites

Xiong Chen,^a Ningh Huang,^a Jia Gao,^a Hong Xu,^a Fei Xu^a and Donglin Jiang^a

^a Department of Materials Molecular Science, Institute for Molecular Science,
National Institutes of Natural Sciences, 5-1 Higashiyama, Myodaiji, Okazaki 444-
8787, Japan.

Corresponding author e-mail: jiang@ims.ac.jp; Tel./Fax: +81 564-59-5520

Contents

Section A. Methods

Section B. Materials and synthetic procedures

Section C. Reaction conditions and XRD patterns

Section D. FT-IR spectral profiles

Section E. Elemental analysis

Section F. FE-SEM images

Section G. TGA profiles

Section H. Structural simulations

Section I. Pore size distribution

Section J. Solid-state electronic absorption spectra

Section K. XRD patterns, porosity, and solid-state electronic absorption of the VO@Py-2,3-DHPh COF

Section L. Stability of the VO@Py-2,3-DHPh COF

Section M. Supporting references

Section A. Methods

^1H and ^{13}C NMR spectra were recorded on JEOL models JNM-LA400 NMR spectrometers, where chemical shifts (δ in ppm) were determined with a residual proton of the solvent as standard. Fourier transform infrared (FT-IR) spectra were recorded on a JASCO model FT-IR-6100 infrared spectrometer. UV-Vis-IR diffuse reflectance spectrum (Kubelka-Munk spectrum) was recorded on a JASCO model V-670 spectrometer equipped with integration sphere model IJN-727. Matrix assisted laser desorption ionization time-of-flight mass (MALDI-TOF-MS) spectra were recorded on an Applied Biosystems BioSpectrometry model Voyager-DE-STR spectrometer in reflector or linear mode using 9-nitroanthracene or dithranol as matrix. Field-emission scanning electron microscopy (FE-SEM) was performed on a JEOL model JSM-6700 operating at an accelerating voltage of 5.0 kV. The sample was prepared by drop-casting a supersonicated dioxane suspension onto mica substrate and then coated with gold. Powder X-ray diffraction (PXRD) data were recorded on a Rigaku model RINT Ultima III diffractometer by depositing powder on glass substrate, from $2\theta = 1.5^\circ$ up to 60° with 0.02° increment. Elemental analysis was performed on a Yanako CHN CORDER MT-6 elemental analyzer.

Inductively coupled plasma atomic emission spectroscopy (ICP-AES) analysis was conducted on a LEEMAN LABS, INC model DRE-100V-R machine. The VO@Py-2,3-DHPh COF samples (2 mg) were placed in a 2-mL polypropylene Eppendorf Safe-Lock centrifuge tube and added with HNO_3 (20 wt%). The tubes were capped and rocked continuously for an hour on a wrist-action shaker (Burrel Scientific, Inc.) before the suspension was removed and filtered. The residual was rinsed with deionized water until the filtrate was 5 mL. This solution was utilized for evaluating the vanadium content.

Nitrogen sorption isotherms were measured at 77 K with a Micromeritics Instrument Corporation model 3Flex surface characterization analyzer. The Brunauer-Emmett-Teller (BET) method was utilized to calculate the specific surface areas. By using the non-local density functional theory (NLDFT) model, the pore volume was derived from the sorption curve.

Molecular modeling and Pawley refinement were carried out using Reflex, a software package for crystal determination from PXRD pattern, implemented in MS modeling ver 4.4 (Accelrys Inc.).^{S1} Unit cell dimension was first manually determined from the observed PXRD peak positions using the coordinates. We performed Pawley refinement to optimize the lattice parameters iteratively until the R_{WP} value converges. The refinement indicates a rhombic orthogonal crystal

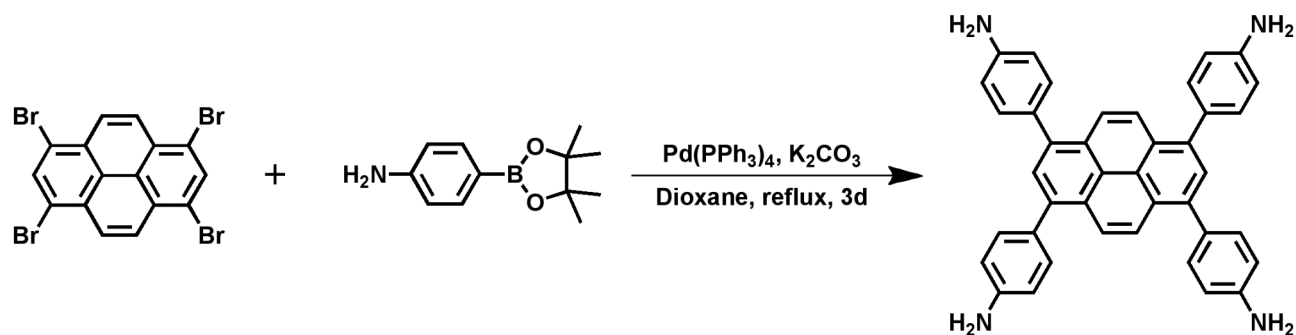
system with a unit cell of $a = 35.82 \text{ \AA}$, $b = 31.90 \text{ \AA}$, and $c = 4.69 \text{ \AA}$; $a = 36.15 \text{ \AA}$, $b = 31.30 \text{ \AA}$, and $c = 3.60 \text{ \AA}$; $a = 42.14 \text{ \AA}$, $b = 36.90 \text{ \AA}$, and $c = 4.33 \text{ \AA}$; and $a = 40.55 \text{ \AA}$, $b = 39.08 \text{ \AA}$, and $c = 3.60 \text{ \AA}$, for the Py-DHPH COF, Py-2,3-DHPH COF, Py-2,2'-BPyPh COF, and Py-3,3'-BPyPh COF, respectively. The pseudo-Voigt profile function was used for whole profile fitting and Berrar-Baldinozzi function was used for asymmetry correction during the refinement processes. The final R_{WP} and R_P values were 8.69% and 7.09%, 10.96% and 9.08%, 10.65% and 8.88%, and 10.93% and 9.10% for the Py-DHPH COF, Py-2,3-DHPH COF, Py-2,2'-BPyPh COF, and Py-3,3'-BPyPh COF, respectively. Simulated XRD patterns were calculated for an AA-stacking and staggered AB-stacking modes. After comparing each simulated pattern with experimentally observed pattern, the AA staking mode yields a pattern that shows good agreement with the observed XRD curve.

Stability of the VO@Py-2,3-DHPH COF samples was conducted by keeping the COFs in different solvents for 24 h, respectively. The resulted samples were washed with THF and acetone, and dried under vacuum at 120 °C overnight.

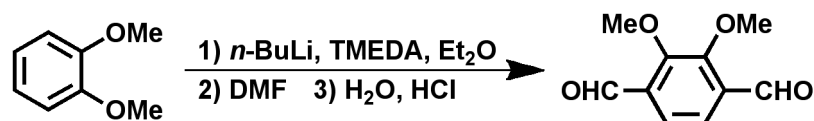
Section B. Materials and synthetic procedures

n-Butanol (*n*-BuOH), *o*-dichlorobenzene (*o*-DCB), anhydrous acetone (99.5%), tetrahydrofuran (THF), mesitylene, dioxane, and acetic acid (AcOH) were purchased from Wako Chemicals. Pyrene, and 4-(4,4,5,5-tetramethyl-1,3,2-dioxaborolan-2-yl)aniline were purchased from Wako Chemicals. 2,5-Dimethoxybenzeneterephthalaldehyde (DMTA), and *t*-butyl lithium solution (1.6 M in pentane) were purchased from Aldrich. Vanadium (IV)-oxy acetylacetonate [VO(acac)₂] was purchased from TCI Chemicals.

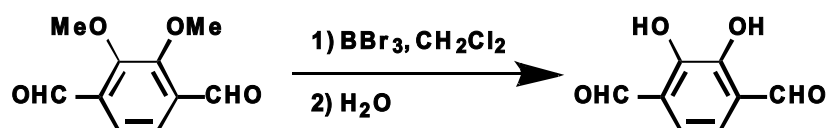
1,3,6,8-Tetrabromopyrene,^{S2} 2,5-dihydroxyterephthalaldehyde (DHTA),^{S3a-c} 2,3-dihydroxyterephthalaldehyde (2,3-DHTA),^{S3b,d} [2,2'-bipyridine]-5,5'-dicarbaldehyde (2,2'-BPyDCA),^{S4} [3,3'-bipyridine]-6,6'-dicarbaldehyde (3,3'-BPyDCA)^{S5} were prepared according to the reported methods.



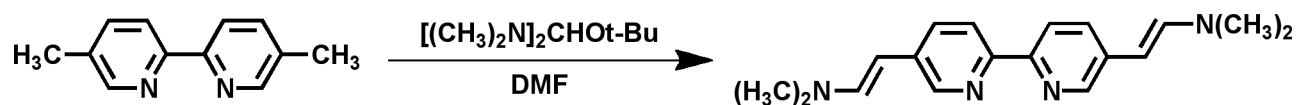
4,4',4'',4'''-(Pyrene-1,3,6,8-tetrayl) tetraaniline (PyTTA). 1,3,6,8-Tetrabromopyrene (500 mg, 0.96 mmol), 4-(4,4,5,5-tetramethyl-1,3,2-dioxaborolan-2-yl)aniline (1.27 g, 5.8 mmol), palladium tetrakis(triphenyl phosphine) (0.06 g, 0.05 mmol), and potassium carbonate (1.05 g, 7.6 mmol) in anhydrous dioxane (15 mL) were stirred under reflux in Ar for 3 days. After cooling to room temperature, the solid was removed by filtration, and washed with acetone for 3 times. The organic phase was evaporated and the crude product was purified by column chromatography over silica gel with chloroform/acetone (9/1 by vol. to pure acetone) eluent. The obtained solid was further purified by recrystallization from chloroform/acetone to afford PyTTA in 61% yield. ¹H NMR (DMSO, 400 MHz): δ (ppm) 8.09 (s, 4H), 7.75 (s, 2H), 7.32-7.29 (d, 8H), 6.74-6.72 (d, 8H), 5.28 (s, 8H). ¹³C NMR (DMSO, 400 MHz): δ (ppm) 148.3, 137.6, 131.6, 129.5, 128.4, 127.2, 126.6, 125.0, 114.7. MALDI-TOF MS for C₄₀H₃₀N₄ (Calc. 566.25), found m/z = 567.17 ([M]⁺).



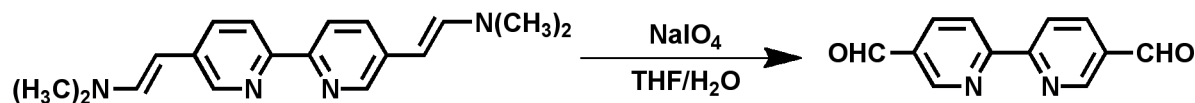
2,3-Dimethoxyterephthalaldehyde (2,3-DMTA).^{S3} Tetramethylethylenediamine (TMEDA) (6.8 mL, 45 mmol) was added to a mixture of 1,2-dimethoxybenzene (1.15 mL, 9 mmol) and diethyl ether (Et₂O, 30 mL), cooled in an ice bath, and added with *n*-butyl lithium (*n*-BuLi, 1.6 M in hexane, 45 mmol) over 10 min. The mixture was stirred in reflux for 10 h. At the end of the metallation, the mixture was cooled to 0 °C, and added with DMF (3.5 mL). After 30 min, the reaction mixture was allowed to warm to room temperature and hydrolyzed with water (50 mL) and aqueous HCl solution (3 M, 10 mL). The organic layer was separated and the aqueous layer was extracted with chloroform three times. The organic layer was dried over MgSO₄, filtered, and concentrated to give reddish brown oil. The residue was then chromatographed on silica gel with chloroform as eluent to give pale yellow solid, which was recrystallized from hexane to afford the target compound in 40% yield. ¹H NMR (CDCl₃, 400 MHz): δ (ppm) 10.45 (s, 2H), 7.64 (s, 2H), 4.06 (s, 6H).



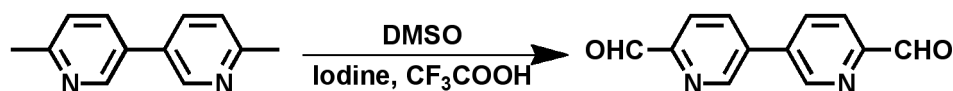
2,3-DHTA.^{S3} To a dichloromethane (CH₂Cl₂, 22 mL) solution of 2,3-DMTA (0.5 g, 2.51 mmol) was added boron tribromide (BBr₃, 1 M in CH₂Cl₂, 10.3 mL) under argon atmosphere. The mixture was stirred for 4 h, added with water (22 mL), and further stirred overnight. The mixture was extracted with CHCl₃, the organic layer was dried over MgSO₄, filtered, and concentrated to dryness. The residue was recrystallized from CH₂Cl₂/hexane to afford the target in 89% yield. ¹H NMR (CDCl₃, 400 MHz): δ (ppm) 10.90 (s, 2H), 10.03 (s, 2H), 7.28 (s, 2H).



(1E, 1'E)-2,2'-([2,2'-Bipyridine]-5,5'-diyl)bis(*N*, *N*-dimethylethenamine).^{S4} Pyrex tube was charged with 5,5'-dimethyl-2,2'-bipyridine (100 mg, 0.54 mmol), DMF (1 mL), and *t*-butoxybis(dimethylamino)methane (1 mL); the reaction mixture was degassed by three freeze-pump-thaw cycles. The tube was sealed and kept in oven at 120 °C for 5 days. On cooling to r.t., yellow crystals were deposited. The crystals were collected, washed with ether (3 × 2 mL), and dried to obtain the target compound in 54% yield. ¹H NMR (CDCl₃, 400 MHz): δ (ppm) 8.39 (s, 2H), 8.11-8.08 (d, 2H), 7.54-7.52 (s, 2H), 6.86-6.83 (d, 2H), 5.11-5.08 (s, 2H), 2.84 (s, 12H).



2,2'-BPyDCA.^{S4} 5,5'-Bis(2-dimethylaminovinyl)-2,2'-bipyridine (100 mg, 0.34 mmol) was dissolved in a mixture of CH₂Cl₂ (4.5 mL) and THF (15 mL). The mixture was added with sodium periodate (0.553 g, 2.6 mmol) in water (3 mL) and stirred at r.t. for 20 h. The solid was filtered off and the solution was concentrated and extracted with CHCl₃. The organic phase was dried over MgSO₄ and evaporated to afford the crude product. The crude product was washed with MeOH to give 2,2'-BPyDCA in 70% yield. ¹H NMR (DMSO, 400 MHz): δ (ppm) 10.16 (s, 2H), 9.20 (s, 2H), 8.65-8.64 (d, 2H), 8.43-8.40 (t, 2H).



3,3'-BPyDCA.^{S5} A solution of 6,6'-dimethyl-3,3'-bipyridine (1 g, 5.43 mmol) in degassed DMSO (40 mL) was prepared in a round-bottom flask. Iodine (2.75 g, 10.86 mmol) was added and the solution was stirred for 10 minutes under Ar. Trifluoroacetic acid (1.17 mL, 15.20 mmol) was added dropwise via syringe. The mixture was refluxed for 3 h at 150 °C under Ar. After cooling to r.t., the reaction was quenched with a 14% aqueous sodium thiosulfate solution and further diluted with a saturated sodium bicarbonate solution. The product was extracted with CH₂Cl₂ (3 × 20 mL), and the organic layer was washed with water and dried over MgSO₄. After filtration, the solvent was evaporated and the solid was washed thoroughly with Et₂O. The product was obtained as beige powder in 20% yield. ¹H NMR (CDCl₃, 400 MHz): δ (ppm) 10.15 (s, 2H), 9.06 (s, 2H), 8.15-8.09 (t, 4H).

Py-DHPh COF. A mesitylene/dioxane/6 M AcOH (5/5/1 by vol.; 1.1 mL) mixture of PyTTA (0.02 mmol, 11.3 mg) and DHTA (0.04 mmol, 6.6 mg) in a Pyrex tube (10 mL) was degassed by three freeze-pump-thaw cycles. The tube was sealed off and heated at 120 °C for 3 days. The precipitate was collected by centrifugation, and washed with anhydrous THF for 5 times and acetone twice. The powder was dried at 120 °C under vacuum overnight to give the Py-DHPh COF in an isolated yield of 80%. The synthesis of the Py-DHPh COF in other solvents, such as *o*-DCB/BuOH/6 M AcOH (5/5/1 by vol.; 1.1 mL), was performed under otherwise same conditions. Elemental analysis (%) calcd. for Py-DHPh COF [(C₅₆H₃₄N₄O₄)_n] C (81.34), H (4.14), and N (6.78), found C (77.25), H (4.57), and N (5.82).

Py-2,3-DHPh COF. A mesitylene/dioxane/6 M AcOH (5/5/1 by vol.; 1.1 mL) mixture of PyTTA (0.02 mmol, 11.3 mg) and 2,3-DHTA (0.04 mmol, 6.6 mg) in a Pyrex tube (10 mL) was degassed by

three freeze-pump-thaw cycles. The tube was sealed off and heated at 120 °C for 3 days. The precipitate was collected by centrifugation, and washed with anhydrous THF for 5 times and acetone twice. The powder was dried at 120 °C under vacuum overnight to give the Py-2,3-DHPh COF in an isolated yield of 85%. The synthesis of the Py-2,3-DHPh COF in other solvents, such as *o*-DCB/BuOH/6 M AcOH (5/5/1 by vol.; 1.1 mL), was performed according to this method under otherwise same conditions. Elemental analysis (%) calcd. for Py-2,3-DHPh COF [(C₅₆H₃₄N₄O₄)_n] C (81.34), H (4.14), and N (6.78), found C (77.69), H (4.33), and N (6.24).

Py-2,2'-BPyPh COF. A mesitylene/dioxane/6 M AcOH (5/5/1 by vol.; 1.1 mL) mixture of PyTTA (0.02 mmol, 11.3 mg) and 2,2'-BPyDCA (0.04 mmol, 8.5 mg) in a Pyrex tube (10 mL) was degassed by three freeze-pump-thaw cycles. The tube was sealed off and heated at 120 °C for 3 or 7 days. The precipitate was collected by centrifugation, and washed with anhydrous THF for 5 times and acetone twice. The powder was dried at 120 °C under vacuum overnight to give the Py-2,2'-BPyPh COF in an isolated yield of 76%. Elemental analysis (%) calcd. for Py-2,2'-BPyPh COF [(C₆₄H₃₈N₈)_n] C (83.64), H (4.17), and N (12.19), found C (77.48), H (5.20), and N (9.53).

Py-3,3'-BPyPh COF. A mesitylene/dioxane/6 M AcOH (5/5/1 by vol.; 1.1 mL) mixture of PyTTA (0.02 mmol, 11.3 mg) and 3,3'-BPyDCA (0.04 mmol, 8.5 mg) in a Pyrex tube (10 mL) was degassed by three freeze-pump-thaw cycles. The tube was sealed off and heated at 120 °C for 3 or 7 days. The precipitate was collected by centrifugation, and washed with anhydrous THF for 5 times and acetone twice. The powder was dried at 120 °C under vacuum overnight to give the Py-3,3'-BPyPh COF in an isolated yield of 78%. Elemental analysis (%) calcd. for Py-3,3'-BPyPh COF [(C₆₄H₃₈N₈)_n] C (83.64), H (4.17), and N (12.19), found C (79.88), H (4.88), and N (10.17).

VO@Py-2,3-DHPh COF. To the as-synthesized Py-2,3-DHPh COF (10 mg, 0.012 mmol) was added with a solution of VO(acac)₂ (50 mg, 189 μmol) in THF (5 mL). The reaction vial was then capped and heated at 50 °C in oil bath for 24 h. The precipitate was isolated via centrifugation, and washed with anhydrous THF for 5 times and acetone twice to remove any excess metal source. The black powder was dried at 120 °C under vacuum overnight to afford the VO@Py-2,3-DHPh COF in a quantitative isolated yield.

Section C. Reaction conditions and XRD patterns

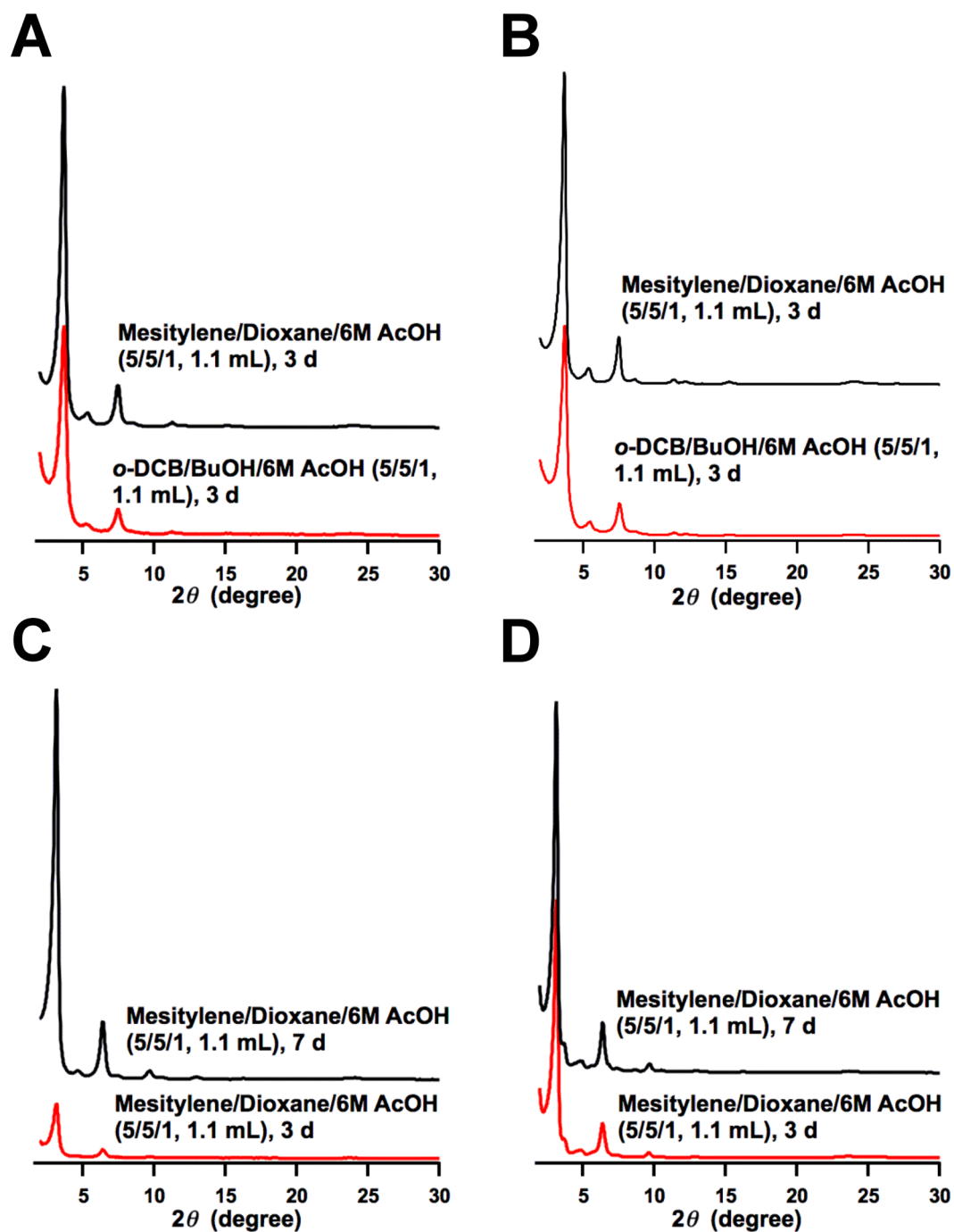


Fig. S1 XRD patterns of (A) Py-DHPh COF, (B) Py-2,3-DHPh COF, (C) Py-2,2'-BPyPh COF, and (D) Py-3,3'-BPyPh COF prepared under different reaction conditions.

Section D. FT-IR spectral profile

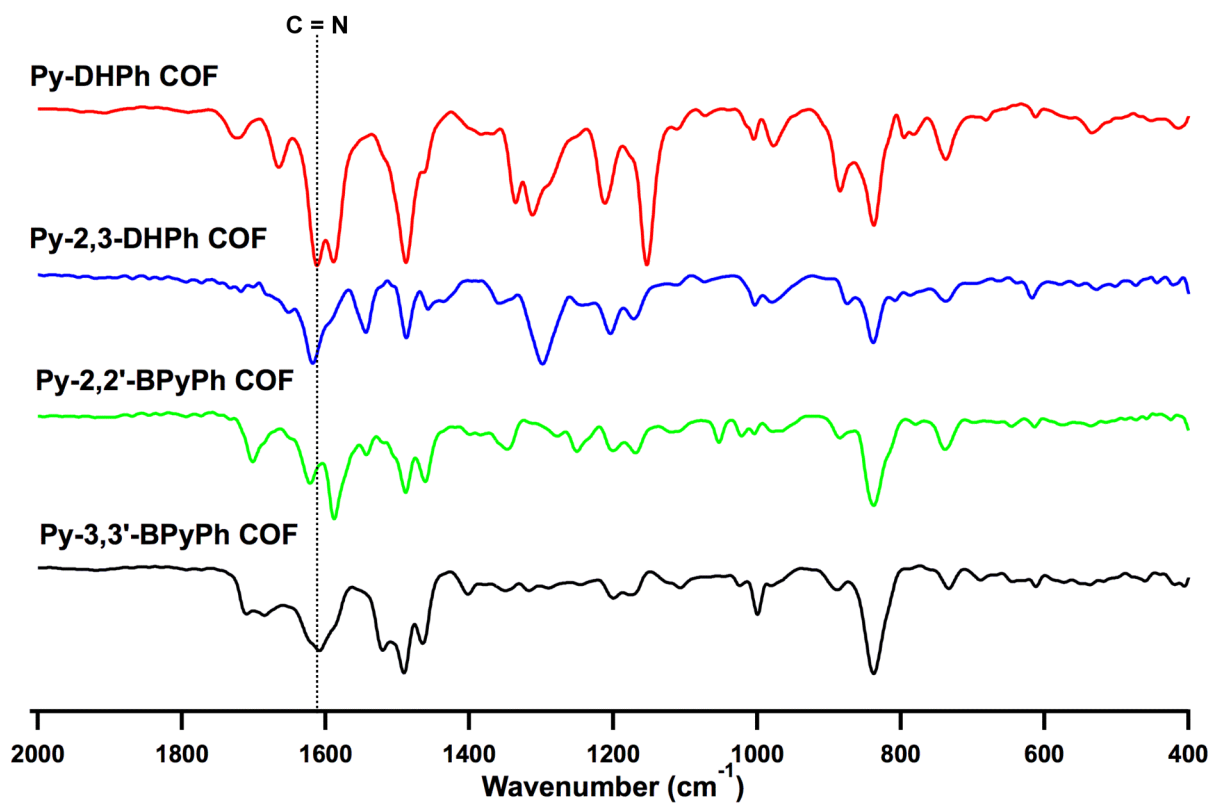


Fig. S2 FT IR spectra of Py-DHPH COF, Py-2,3-DHPH COF, Py-2,2'-BPyPh COF, and Py-3,3'-BPyPh COF.

Table S1. The C=N vibration bands of the COFs

Compound	C=N (cm ⁻¹)
Py-DHPH COF	1612
Py-2,3-DHPH COF	1618
Py-2,2'-BPyPh COF	1622
Py-3,3'-BPyPh COF	1608

Section E. Elemental analysis

Table S2. Elemental analysis.

COFs		C %	H %	N %
Py-DHPh COF	Calcd.	81.34	4.14	6.78
	Found	77.25	4.57	5.82
Py-2,3-DHPh COF	Calcd.	81.34	4.14	6.78
	Found	77.69	4.33	6.24
Py-2,2'-BPyPh COF	Calcd.	83.64	4.17	12.19
	Found	77.48	5.20	9.53
Py-3,3'-BPyPh COF	Calcd.	83.64	4.17	12.19
	Found	79.88	4.88	10.17

Section F. FE-SEM images

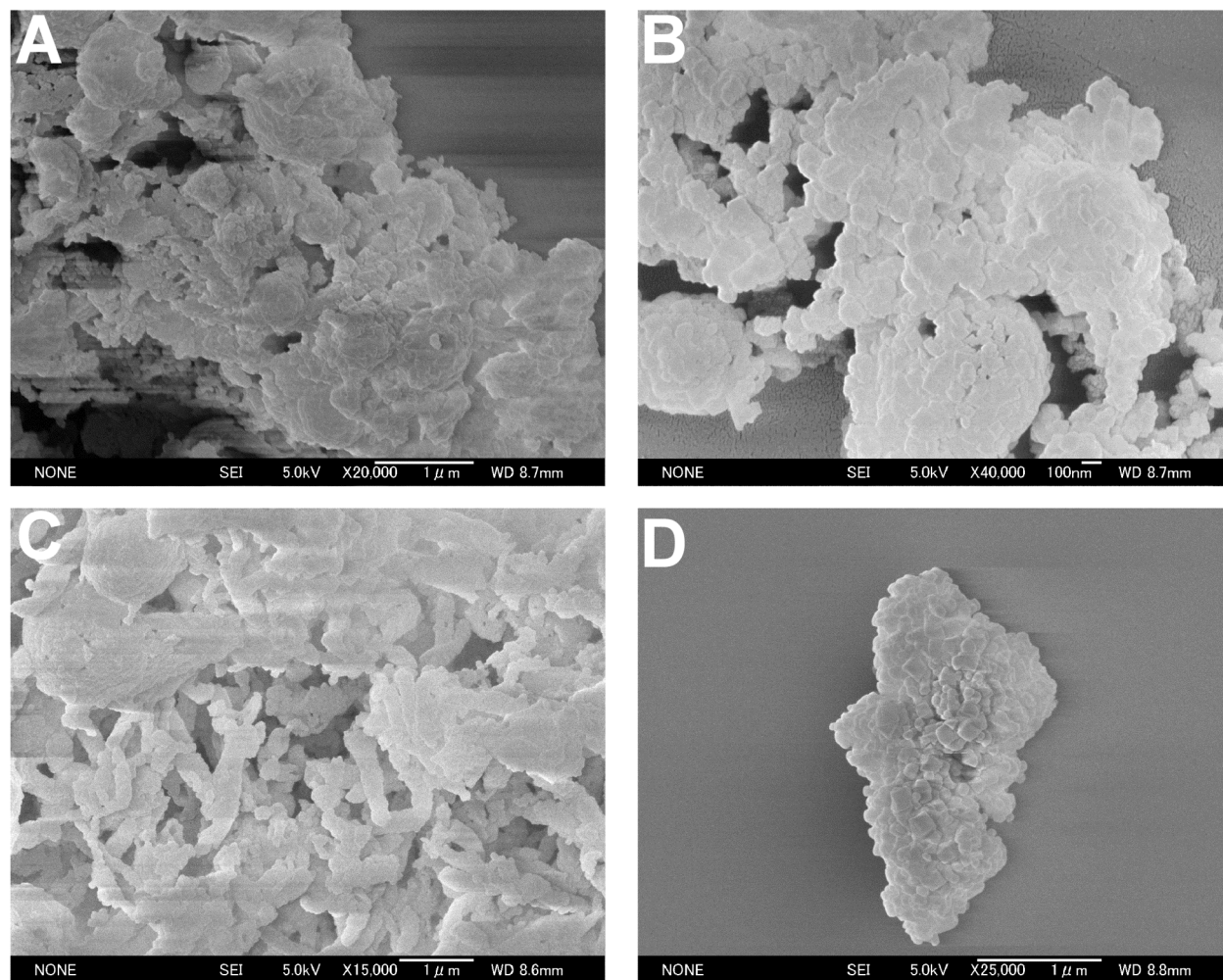


Fig. S3 FE-SEM images of (A) Py-DHPH COF, (B) Py-2,3-DHPH COF, (C) Py-2,2'-BPyPh COF, and (D) Py-3,3'-BPyPh COF.

Section G. TGA profiles

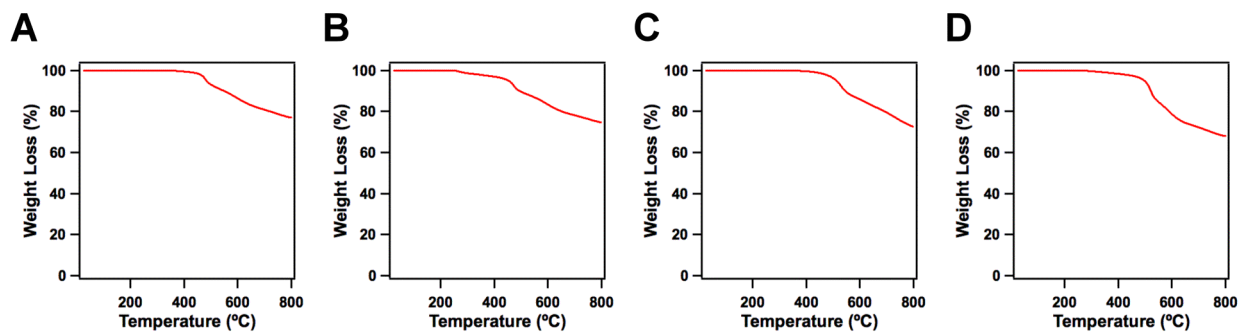


Fig. S4 TGA curves of (A) Py-DHPH COF, (B) Py-2,3-DHPH COF, (C) Py-2,2'-BPyPh COF, and (D) Py-3,3'-BPyPh COF.

Section H. Structural simulations

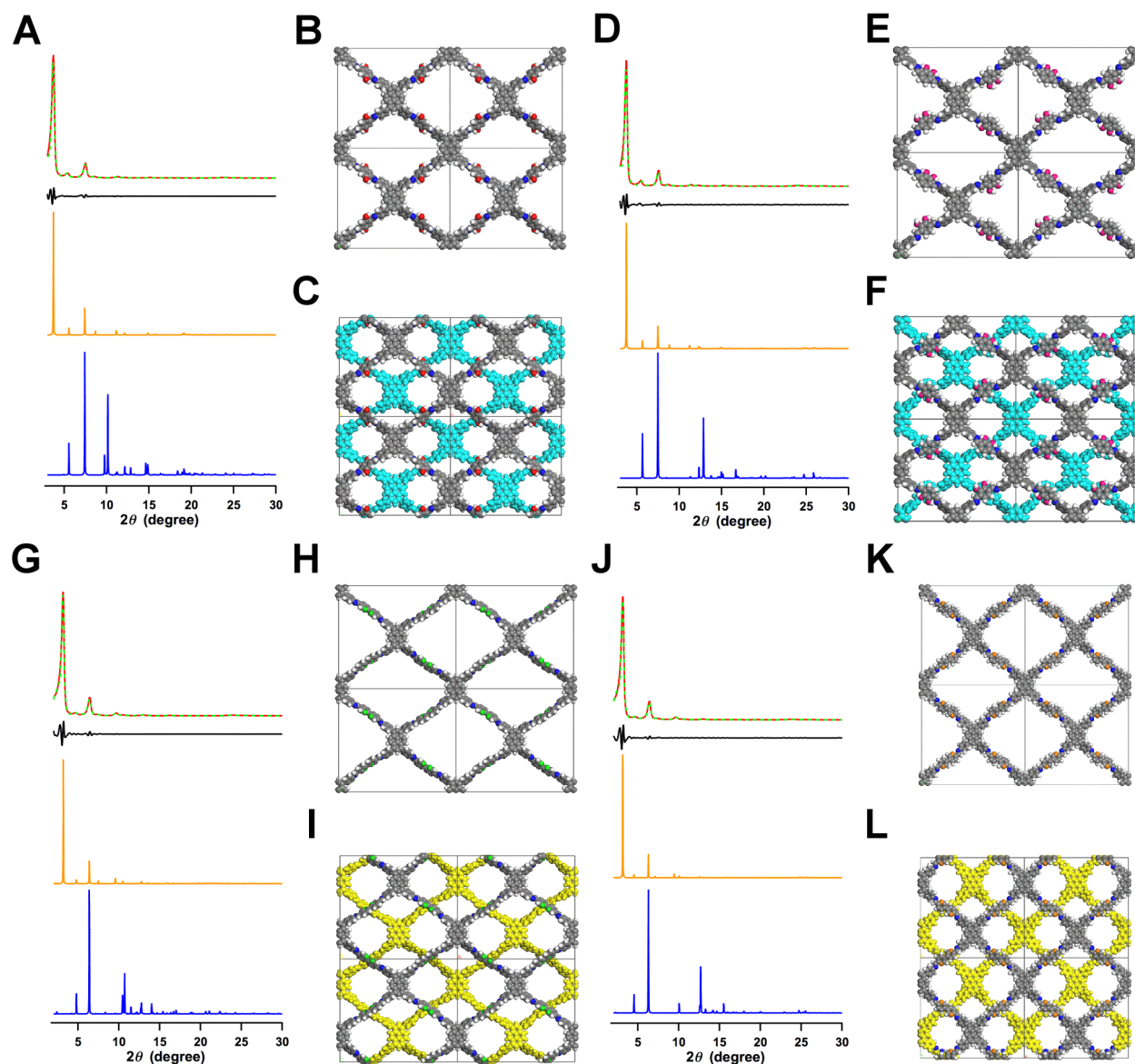


Fig. S5 XRD patterns of (A) Py-DHPH COF, (D) Py-2,3-DHPH COF, (G) Py-2,2'-BPyPh COF, and (J) Py-3,3'-BPyPh COF (experimental (red), Pawley refinement (green dotted line), difference between experimental and Pawley refined data (black), simulated XRD patterns using the AA stacking mode (orange) and staggered AB stacking mode (blue)). Unit cells of the AA stacking modes of (B) Py-DHPH COF, (E) Py-2,3-DHPH COF, (H) Py-2,2'-BPyPh COF, and (K) Py-3,3'-BPyPh COF. Unit cells of the staggered AB stacking modes of (C) Py-DHPH COF, (F) Py-2,3-DHPH COF, (I) Py-2,2'-BPyPh COF, and (L) Py-3,3'-BPyPh COF.

Table S3. Pawley refined crystal unit cell parameters.

COFs	Space group	Unit cell parameters	R_{WP} and R_P values
Py-DHPh COF	$PMMN$	$a = 35.82 \text{ \AA}, b = 31.90 \text{ \AA}, c = 4.69 \text{ \AA}, \alpha = \beta = \gamma = 90^\circ$	$R_{WP} = 8.69\%, R_P = 7.09\%$
Py-2,3-DHPh COF	$PMM2$	$a = 36.15 \text{ \AA}, b = 31.30 \text{ \AA}, c = 3.60 \text{ \AA}, \alpha = \beta = \gamma = 90^\circ$	$R_{WP} = 10.96\%, R_P = 9.08\%$
Py-2,2'-BPyPh COF	$PMM2$	$a = 42.14 \text{ \AA}, b = 36.90 \text{ \AA}, c = 4.33 \text{ \AA}, \alpha = \beta = \gamma = 90^\circ$	$R_{WP} = 10.65\%, R_P = 8.88\%$
Py-3,3'-BPyPh COF	$P222$	$a = 40.55 \text{ \AA}, b = 39.08 \text{ \AA}, c = 3.60 \text{ \AA}, \alpha = \beta = \gamma = 90^\circ$	$R_{WP} = 10.93\%, R_P = 9.10\%$

Section I. Pore size distribution

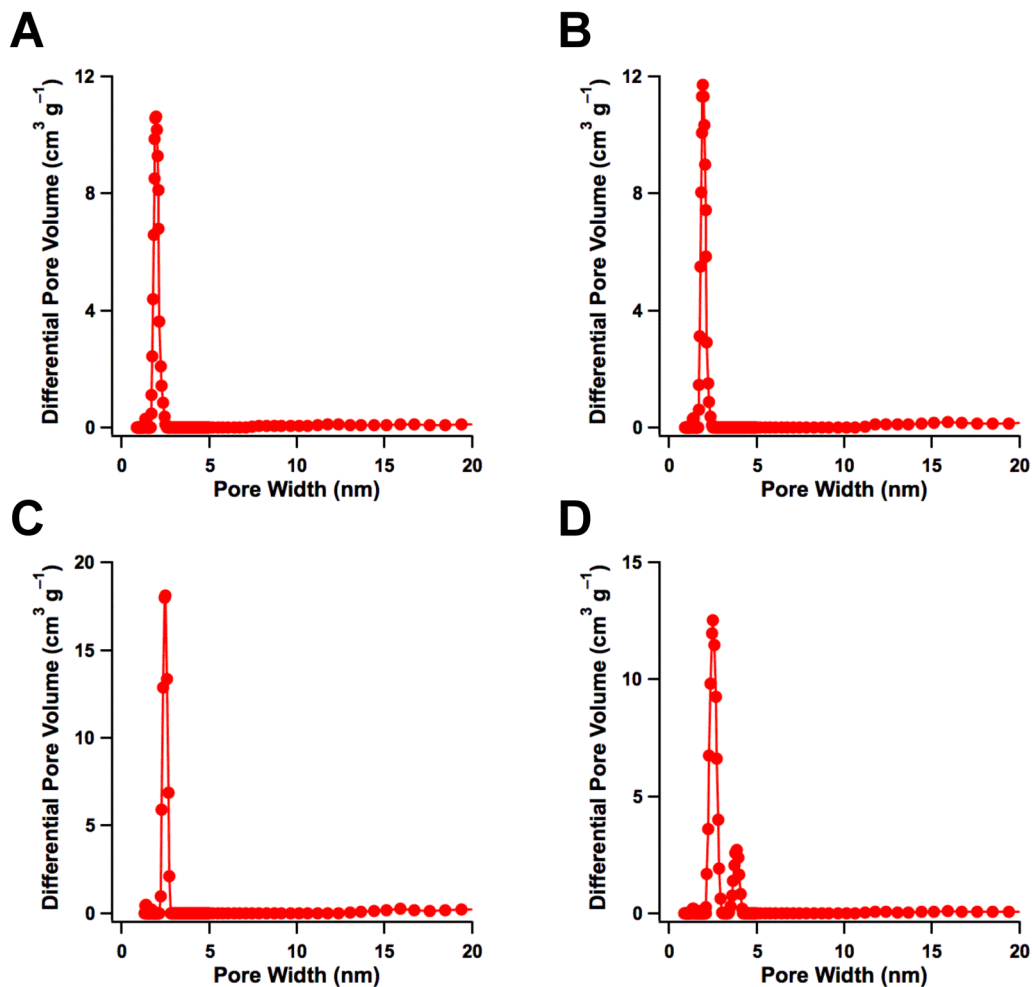


Fig. S6 Pore size distributions of (A) Py-DHPPh COF, (B) Py-2,3-DHPPh COF, (C) Py-2,2'-BPyPh COF, and (D) Py-3,3'-BPyPh COF. The small peak at 3.8 nm in Figure S6d is likely attributed to the pore defect and edge parts; its contribution to the surface area is about 10%.

Table S4. Total pore volumes of the COFs.

COF	Total pore volume (V_P , $\text{cm}^3 \text{g}^{-1}$)
Py-DHPH COF	1.45
Py-2,3-DHPH COF	1.51
Py-2,2'-BPyPh COF	1.85
Py-3,3'-BPyPh COF	1.49

Section J. Solid-state electronic absorption spectra

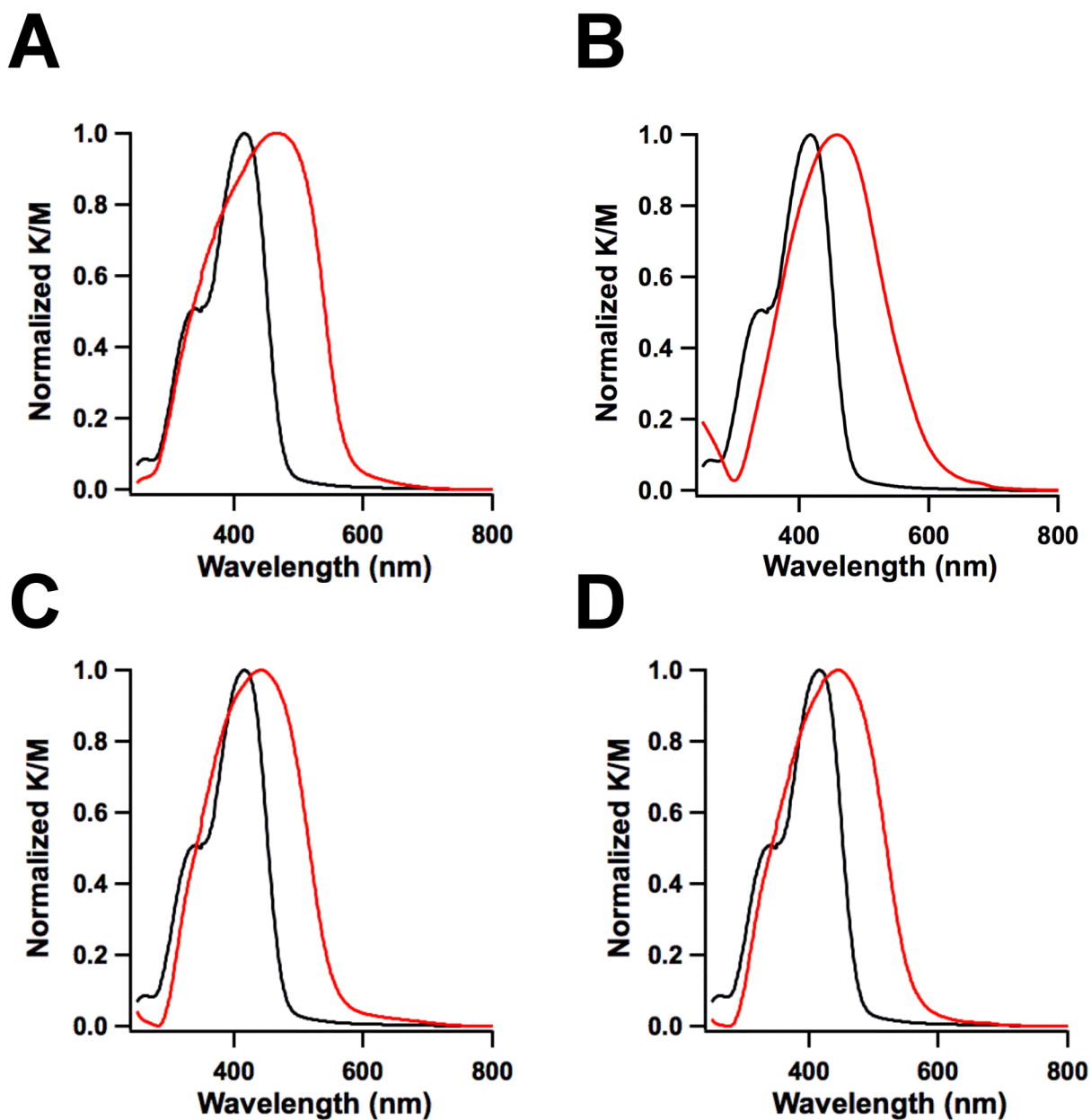


Fig. S7 Solid-state electronic absorption spectra of (A) Py-DHPh COF, (B) Py-2,3-DHPh COF, (C) Py-2,2'-BPyPh COF, and (D) Py-3,3'-BPyPh COF (red curves). The spectrum of PyTTA monomer was showed in black.

Section K. XRD patterns, porosity, and solid-state electronic absorption of the VO@Py-2,3-DHPH COF

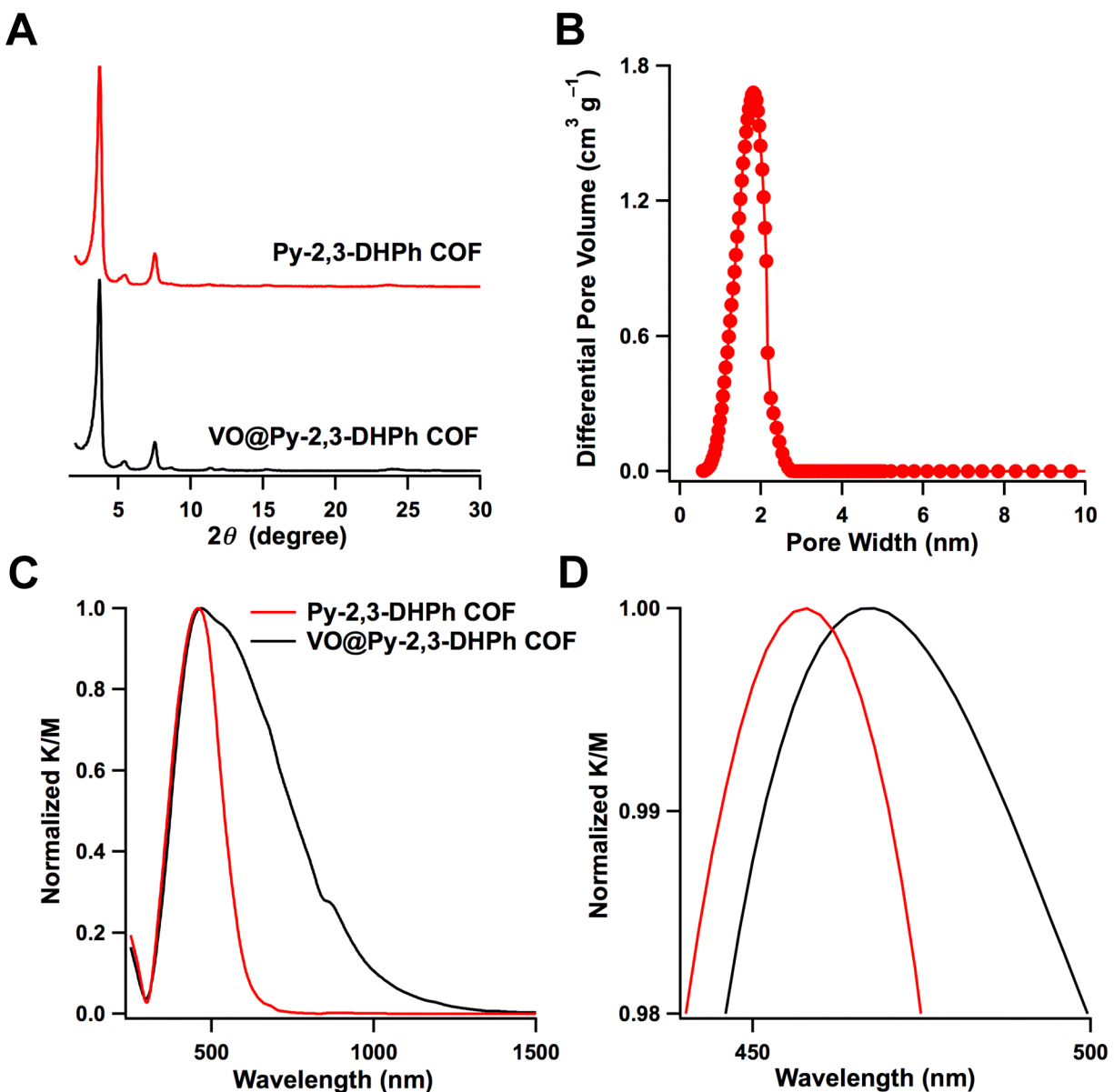


Fig. S8 (A) XRD patterns of the Py-2,3-DHPH COF (red) and VO@Py-2,3-DHPH COF (black), (B) Pore size distribution of VO@Py-2,3-DHPH COF, (C) Solid-state and (D) enlarged electronic absorption spectra of Py-2,3-DHPH COF (red) and VO@Py-2,3-DHPH COF (black).

Section L. Stability of the VO@Py-2,3-DHPH COF

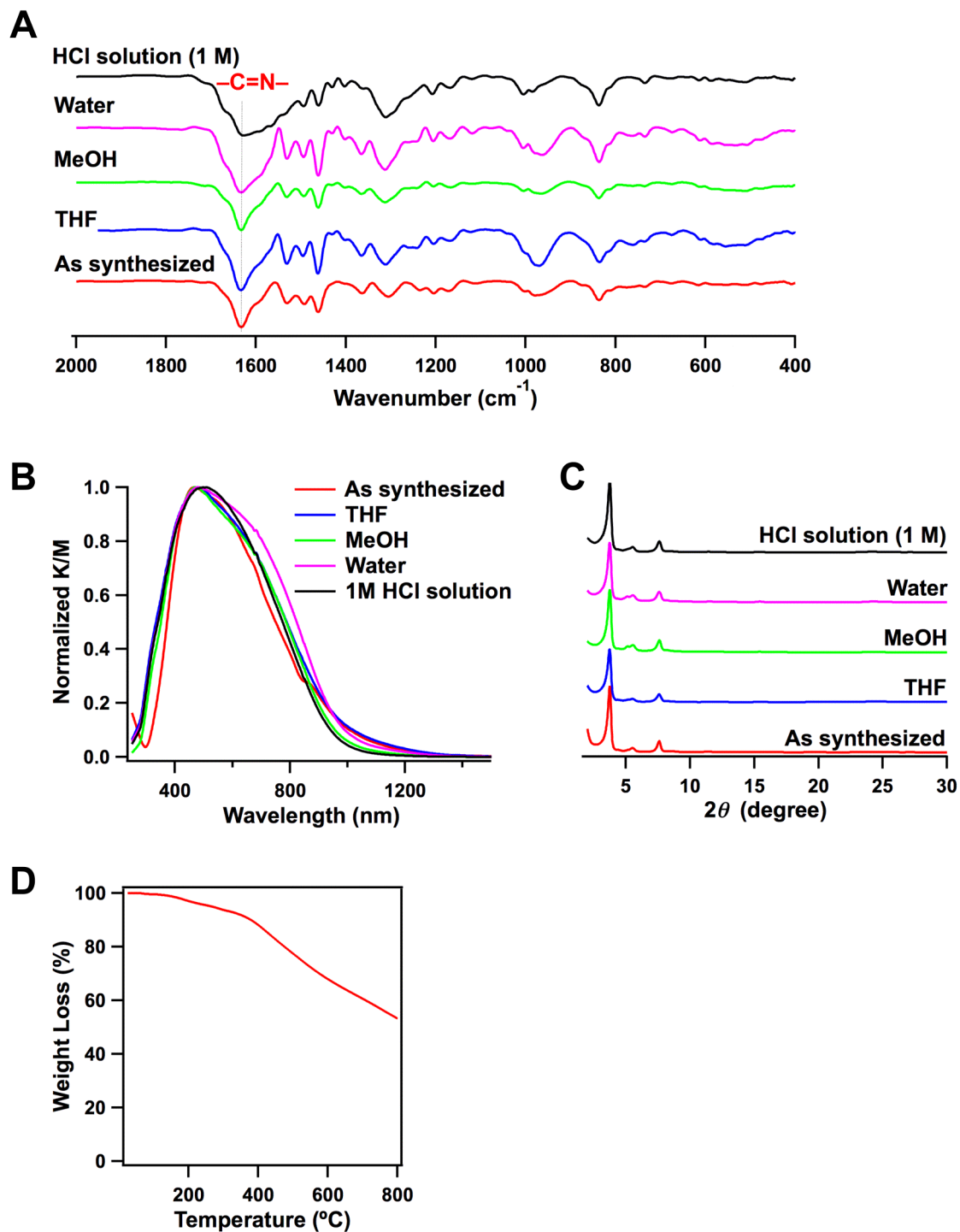


Fig. S9 (A) IR and (B) electronic absorption spectra, and (C) XRD patterns of the VO@Py-2,3-DHPH COF samples upon 24-h treatment in different solvents. (D) TGA curve of the VO@Py-2,3-DHPH COF.

Section M. Supporting References

S1 Accelrys, Material Studio Release Notes, Release 4.4, Accelrys Software, San Diego 2008.

S2 M. G. Rabbani, A. K. Sekizkardes, O. M. El-Kadri, B. R. Kaafarani, H. M. El-Kaderi, *J. Mater. Chem.* 2012, **22**, 25409-25417.

S3 (a) A. Palmgren, A. Thorarensen, J. Bäckvall, *J. Org. Chem.* 1998, **63**, 3764-3768. (b) N. Kuhnert, G. M. Rossignolo, A. L. Periago, *Org. Biomol. Chem.*, 2003, **1**, 1157-1170. (c) T. Kretz, J. W. Bats, H. W. Lerner, T. Z. Wagner, *Naturforsch.* 2007, **62b**, 66-74. (d) S. Akine, T. Taniguchi, T. Nabeshima, *J. Am. Chem. Soc.* 2006, **128**, 15765-15774.

S4 J. Hodačová, M. Buděšínský, *Org. Lett.* 2007, **9**, 5641-5643.

S5 A. Muppidi, Z. Wang, X. Li, J. Chen, Q. Lin, *Chem. Commun.*, 2011, **47**, 9396-9398.